



## Numerical Investigation of Inverse Curvature Ogee Spillway

Rasoul Daneshfaraz <sup>a\*</sup>, Amir Ghaderi <sup>b</sup>

<sup>a</sup> Associate Professor, Department Of Civil Engineering, University of Maragheh, Maragheh, Iran.

<sup>b</sup> Ph.D. student of Civil engineering-Hydraulic structures, University of Zanjan, Iran.

Received 21 October 2017; Accepted 30 November 2017

### Abstract

Design of water structures and their segments including spillways play an important role in water resources management and agricultural activities. In the the linear body part of an ogee spillway, for speeding up the flow rate, the flow should be transferred to the stilling basin by inverse curve so that the water energy can be reduced. This study aims to evaluate the effect of the inverse profile curvature on the pressure of spillway surface using Fluent software. For this purpose, five different curvatures of inverse profile were considered to be equal to no-curvature (zero), 1, 1.5, 2 and 2.5 of the spillway design head. The results indicated that by increasing the curvature radius, the maximum pressure dramatically reduced. And for this purpose, some relationships were given to predict the pressure reduction. Pressure increment in zero curvature is caused by sudden collision of flow lines and turbulence caused by it. By increase in inverse profile curvature, the turbulence is created in flow lines and the maximum pressure shows a lower value than before. In general, there was little change in the average absolute pressure.

*Keywords:* Numerical Modeling; Ogee Spillway; Pressure Profile; Inverse Curvature.

### 1. Introduction

Ogee spillway is one of the most common yet the least expensive spillways which can pass large amount of water. This spillway is composed of different parts. One of the important segments of these spillways that was less investigated by researchers is the inverse curvature at the end of the ogee spillway which transfers the flow on the spillway profile to the stilling basin. These spillways are often used in diversion weirs due to high hydraulic efficiency.

Many studies are implemented in the field of experimental and numerical design of ogee spillways. One of the issues raised due to the falling jet effect on downstream of hydraulic structures are energy dissipation and erosion. An important parameter in hydraulic systems is control of flow rate and pressure on the spillway [1]. Bradley (1945), defined four distinct types of flows over spillways. Flow type I is a rapid flow with supercritical regime; type 2 has a stationary hydraulic jump; flow type 3 includes submerged jump and type 4 describes the spillway submergence [2]. Cassidy (1965) applied Laplace equation for the first time using finite difference method for flow analysis on ogee spillway Using potential flow theory, he examined the flow pressure on spillways and free surface of water and verified his numerical model with the use of laboratory results [3]. Maynord (1985) examined a simple way to design the ogee spillway crest curve. He measured the discharge coefficient and static pressure on the crest as well as the water surface profile both with and without base, and presented their results in graphs and tables. He came to the conclusion that low spillway height and broad crest have the same discharge characteristics [4]. Savage and Johnson (2001) modeled the flow over an ogee spillway physically and numerically and also compared their results with the data on the USBR and USACE. For comparison, they used dimensionless discharge curves and achieved a good agreement in physical and numerical results [5]. Chunrong et al. (2002) used fluid volume method to simulate the flow in circular crest spillways. Then, the

\* Corresponding author: daneshfaraz@yahoo.com

 <http://dx.doi.org/10.28991/cej-030944>

➤ This is an open access article under the CC-BY license (<https://creativecommons.org/licenses/by/4.0/>).

© Authors retain all copyrights.

results of numerical simulations were compared with experimental results. The results showed good agreement between the numerical and experimental results [6]. Chatila and Tabara (2004) modeled water surface profiles over ogee spillways, using computational fluid dynamics of finite element software (ADINA) and  $k-\varepsilon$  turbulence model. Their calculations showed a reasonable agreement with experimental results [7]. Johnson and Savage (2006) studied experimental and numerical results of the flow over ogee spillways considering the effect of tailwater. Comparison of their results showed that there is a good agreement between experimental and numerical results and that the numerical solution can simulate the flow over the spillway well and pressure distribution on the spillway. Hence, it is a useful software for simulation of hydraulic structures such as dams and spillways [8].

Tullis (2010) reviewed the discharge coefficient of submerged ogee spillways. He re-examined the proposed method to predict the discharge coefficient by USBR and compared the results of this method with the results of his experiments for 9 different geometries of ogee spillway and a wide range of submerged flows. According to Tullis, there is a relatively poor compatibility between his laboratory results and the results obtained by USBR method. So, he has offered alternative relations to predict the discharge coefficient of submerged ogee spillways [9]. Vosoughifar and Daneshkhah (2010) conducted a numerical study of the flow over ogee spillways with Fluent software. Using the Froude number obtained from simulations in different parts of the spillway, they determined the range of flow regimes in those points. Their results showed that reduction in the design head, increase the average rate of the flow over spillway consequently, the Froude number also decreases [10]. Morales et al. (2012) conducted a numerical and physical modeling of ogee spillway with radial valve of the Connor River diversion dam in Ecuador. Water surface profiles and the relative rate were compared in two models and a good agreement between these two methods was achieved [11]. Alhashimi (2013) conducted a numerical study of the flow over the ogee spillway with different turbulence models. He used Fluent software to perform simulations. His results showed that results of the numerical solution with  $k-\varepsilon$  turbulence model have a high accuracy compared to other turbulence models and are closer to experimental results [12].

Daneshfaraz et al. (2014) conducted a numerical study of the flow over stepped and ogee spillways with finite volume and finite element. In that study, they compared two discretization methods in numerical solution through FLUENT and ADINA softwares and also compared the results with experimental data. Finding good agreement between experimental and numerical results. Meantime, results of the limited volume of Fluent software were more accurate than the finite element of ADINA software [13]. Herrera Granados and Kostecki (2016) also conducted an experimental and numerical study of flow over ogee spillway. It was about Niedów barrage in the southern Poland. Their aim was to evaluate the spillway discharge floods. Their results showed a good agreement between the numerical and experimental results. As well, the dam with an ogee spillway had the potential of flood evacuation in the event of catastrophic flooding [14]. Daneshfaraz et al. (2016) adopted standard  $k-\varepsilon$ , renormalization group  $k-\varepsilon$ , and standard  $k-\omega$  turbulence model to simulate the four step arrangements stepped spillways. And pressure distribution was studied by RNG  $k-\varepsilon$  turbulence model, which was regarded as the optimal turbulence model through comparing the physical value and numerical value of water level [15].

In spite of numerous studies which have been dedicated to numerical simulation of flow over ogee spillways, the effect of inverse curve on flow parameters such as pressure is less than clear cut. In this study, the flow over ogee spillway was simulated 2 dimensionally using Fluent software. After studying the simulation results and comparing them with experimental results (Chatila and Tabara, 2004), different inverse curvature profiles were suggested. Numerical simulation was also performed for each of the profiles and the results were discussed.

## 2. Materials and Methods

### 2.1. Governing Equations

Equations governing a viscous incompressible fluid in a turbulent state are expressed by in depth averaged Navier-Stokes equations, so called Reynolds, which include the equations of continuity and motion [16].

$$\frac{\partial \rho}{\partial t} + \frac{\partial(\rho u_i)}{\partial x_i} = 0 \quad (1)$$

$$\frac{\partial u_i}{\partial t} + u_j \frac{\partial u_i}{\partial x_j} = -\frac{1}{\rho} \frac{\partial P}{\partial x_i} + g_i + \frac{\partial}{\partial x_j} S_{ij} \quad (2)$$

In the above equations  $u_i$  is the rate factor in the direction  $x_i$ ,  $P$  is the total pressure,  $\rho$  is the fluid density,  $g_i$  is the velocity gravity in  $x_i$  direction,  $S_{ij}$  is the stress tensor. These can be expressed as the following equation for the turbulent flow [16].

$$S_{ij} = \left[ \rho(v + v_t) \left( \frac{\partial u_i}{\partial x_j} + \frac{\partial u_j}{\partial x_i} \right) \right] - \left[ \frac{2}{3} \rho(k + v_t) \frac{\partial u_i}{\partial x_i} \delta_{ij} \right] \quad (3)$$

In the above equations,  $v_t$  is the eddy viscosity which is a function of flow and turbulence characteristics.  $\delta_{ij}$  is used for application of eddy viscosity definition. Turbulent kinetic energy per mass unit is expressed by equation 5.

$$\delta_{ij} = \begin{cases} 1 & i = j \\ 0 & i \neq j \end{cases} \quad (4)$$

$$k = \frac{1}{2} \left( \overline{u_i^2} + \overline{u_j^2} + \overline{u_k^2} \right) \quad (5)$$

## 2.2. Numerical Model

In this paper, Fluent Software has been used to study the physical properties of flow over ogee spillways. For this purpose, it is required to plot the geometry of model and meshing using GAMBIT software. Fluent is a multipurpose software used for the modeling of fluid flow, transfer of heat and chemical reactions. It has the capability of analyzing complicated and turbulent flows and it is based on finite volume method, which is a very strong method to solve computational fluid dynamics [10]. It should be noted that the volume of fluid (VOF) is used in this study to obtain water surface profiles. The variable function of  $\alpha$  is used in VOF method which is a part of water volume in the computational cell. If  $\alpha$  is equal to 1, it represents a cell full of water and if  $\alpha$  is equal to zero, it means that there is no air in the cell. For  $1 < \alpha < 0$ , alpha represents the fullness percentage of the cell. Therefore by considering the free surface in a given volume fraction, the free surface flow can be determined. The amount of  $\alpha$  for determining the water surface profile is usually equal to 0.5 as prescribed value [17].

A turbulence model is needed for additional modeling of nonlinear Reynolds stress term. For this purpose, the RNG\* k- $\epsilon$  turbulence model is used in this study to simulate mean flow characteristics for turbulent flow conditions. the RNG k- $\epsilon$  could couple successfully with a large number of meshes. It has been utilized successfully in the similar numerical studies which simulated Flow through the weir [15, 18-20].

The RNG k- $\epsilon$  model is a two-equation turbulence model. The first equation (Equation 6) determines the energy in the turbulence and is called turbulent kinetic energy (k) and the second equation (Equation 7) is the turbulent dissipation ( $\epsilon$ ), which determines the rate of dissipation of the turbulent kinetic energy.

$$\frac{\partial(\rho k)}{\partial t} + \frac{\partial(\rho k u_i)}{\partial x_i} = \frac{\partial}{\partial x_j} \left[ \left( \mu + \frac{\mu_t}{\sigma_k} \right) \frac{\partial k}{\partial x_j} \right] + P_k - \rho \epsilon \quad (6)$$

$$\frac{\partial(\rho \epsilon)}{\partial t} + \frac{\partial(\rho \epsilon u_i)}{\partial x_i} = \frac{\partial}{\partial x_j} \left[ \left( \mu + \frac{\mu_t}{\sigma_\epsilon} \right) \frac{\partial \epsilon}{\partial x_j} \right] + C_{1\epsilon} \frac{\epsilon}{k} P_k - C_{2\epsilon}^* \rho \frac{\epsilon^2}{k} \quad (7)$$

In which:

$$C_{2\epsilon}^* = C_{2\epsilon} + \frac{C_\mu \eta^3 (1 - \eta / \eta_0)}{1 + \beta \eta^3} \quad (8)$$

$$\eta = \frac{S k}{\epsilon} \quad (9)$$

$$S = \sqrt{2 S_{ij} S_{ij}} \quad (10)$$

$$S_{ij} = \frac{1}{2} \left( \frac{\partial u_i}{\partial x_j} + \frac{\partial u_j}{\partial x_i} \right) \quad (11)$$

In the RNG k- $\epsilon$  turbulence model,  $C_\mu = 0.0845$ ;  $C_{1\epsilon} = 1.42$ ;  $C_{2\epsilon} = 1.68$ ;  $\sigma_k = 0.7194$ ;  $\sigma_\epsilon = 0.7194$ ;  $\eta_0 = 4.38$ ; and  $\beta = 0.012$ . These adjustable constants have been arrived by data fitting a wide range of turbulent flows [21].

\* Re-Normalization Group

**2.3. The Model Geometry, Meshing, and Boundary Conditions**

Ogee spillway profile body designed based on the design table 111-2/1 of USACE-WES. Spillway body components include an upstream vertical plane (Part 1 in Figure 1), two arcs with curvature radii of  $0.2H_d$  and  $0.5H_d$  in the spillway crest (Part 2 and 3 in Figure 1), spillway curve obtained by equation 6 (part 4 in Figure 1), the linear part (part 5 in Figure 1), and the inverse curve for transferring the flow from the spillway body into the stilling basin (part 6 in Figure 1).

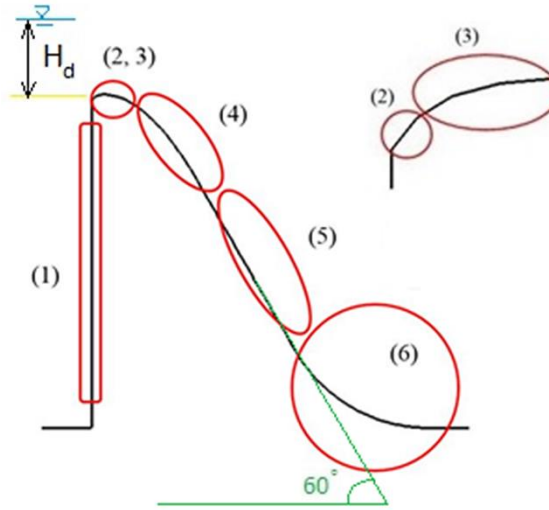


**Figure 1. Different segments of the spillway profile body**

Spillway body is defined by the equation  $x^n = KH_d^{1-n}y$  which is completed by the coefficients  $K = 2, n = 1.85,$  and  $H_d = 5.08 \text{ cm}.$  It should be noted that in the above equations,  $H_d$  is the spillway design head (Hydraulic Design Criteria), and the linear part of the spillway body has a slope of 60 degrees (or slope of 1.73:1). Equation 6 defines spillway profile for the segment 2 in Figure 1 [9].

$$y = 0.1256x^{1.85} \tag{6}$$

Mesh generation was done by GAMBIT software. As shown in Figure 2, a 2D grid was used for mesh generation which quadrilateral mesh is selected (Due to the geometry of spillway, Map mesh was used in some areas and Pave mesh was used in some other areas). Mesh sizes in areas such as the spillway profiles surface, where changes in the values of parameters such as pressure were important, were considered much smaller than other points. This also helped to increase the speed of analysis. Figure 3 shows the meshing details of ogee spillway for the case where the inverse curve radius is equal to the spillway design head. In table 1, meshing details, number of meshes, water head, and input rate are shown in all cases of the inverse curve. Although different alternative mesh was evaluated in the first stage of research, this type of mesh was selected regarding to runtime and error between computed and observed water surface profile.

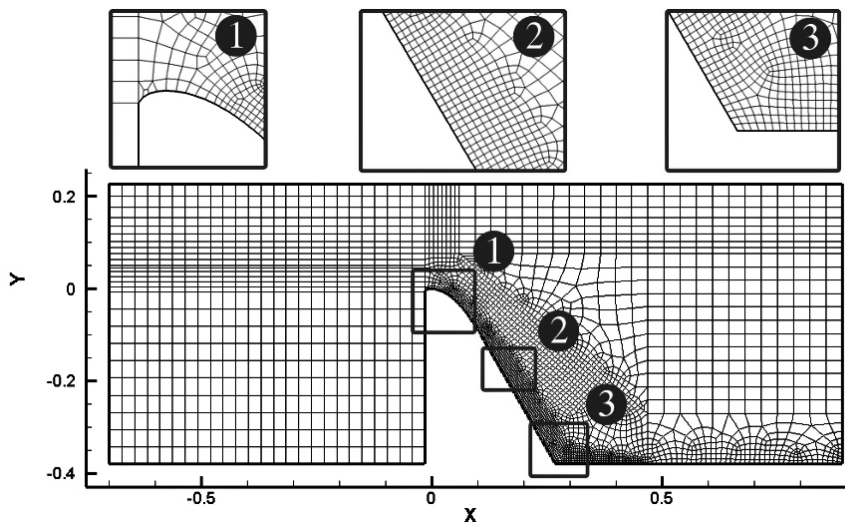


**Figure 2. Meshing details of the spillway without an inverse curve**

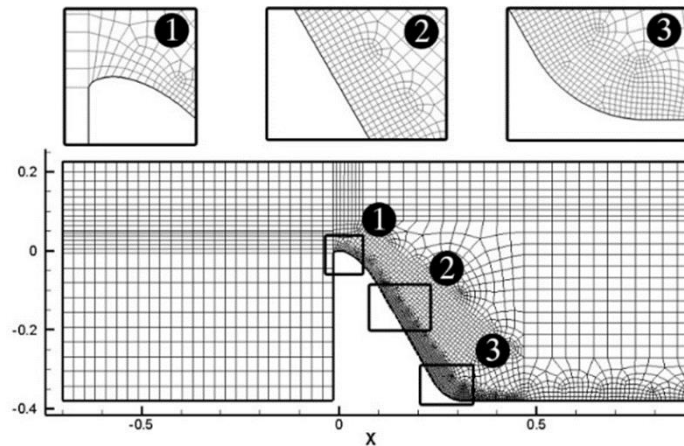


Figure 3. Meshing details of the spillway with a curve of radius equal to the spillway design head

Table 1. Details of spillway simulation in all cases of inverse curve

No	Head/ $H_d$	Number of cells					Flow velocity (m/s)
		$r/H_d=0$	$r/H_d=1$	$r/H_d=1.5$	$r/H_d=2$	$r/H_d=2.5$	
1	1.5	3950	3939	4014	3897	3861	0.1025
2	1	3950	3939	4014	3897	3861	0.05539
3	0.75	3950	3939	4014	3897	3861	0.03566

Where  $r$  is the radius of curvature and  $H_d$  is the head passing over the spillway. In general, one of the most important phases of the numerical analysis of flow field is to determine proper boundary conditions, which are matched appropriately with the physical conditions of the problem. The boundary conditions used in the simulation of this study are shown in Figure 4. In this Figure, the input boundaries are the rates which include water input flow rate and air input flow rate. The input values of water flow rate were 0.1025, 0.0553, 0.0356 m/s and the air input value is considered as the negligible, amount of 0.00001 m/s. Pressure boundary conditions were also shown as input and output in the Figure. Boundaries on the floor constitute the wall boundary conditions or fixed wall where non-slip condition is considered in Fluent software default for this type of boundary.

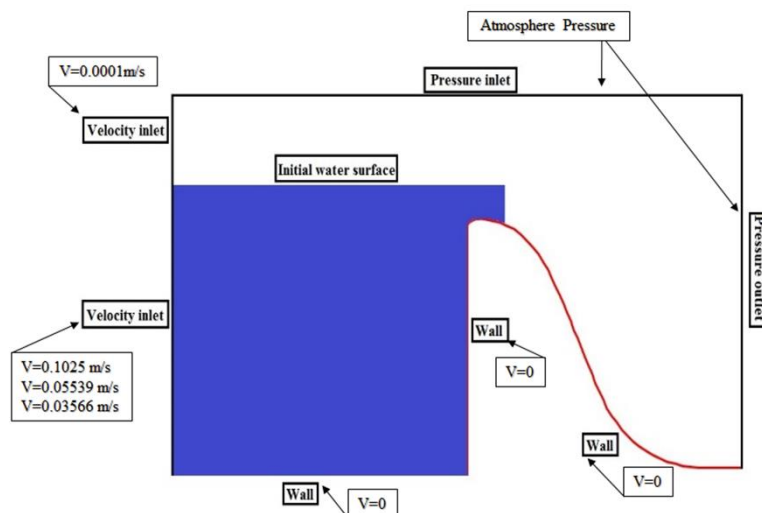


Figure 4. Boundary conditions governing the issue

In Figure 5, water and air contours are shown in solution range after 4 seconds. It should be noted that the numbers marked with a color spectrum are indicative of the  $\alpha$  parameter.

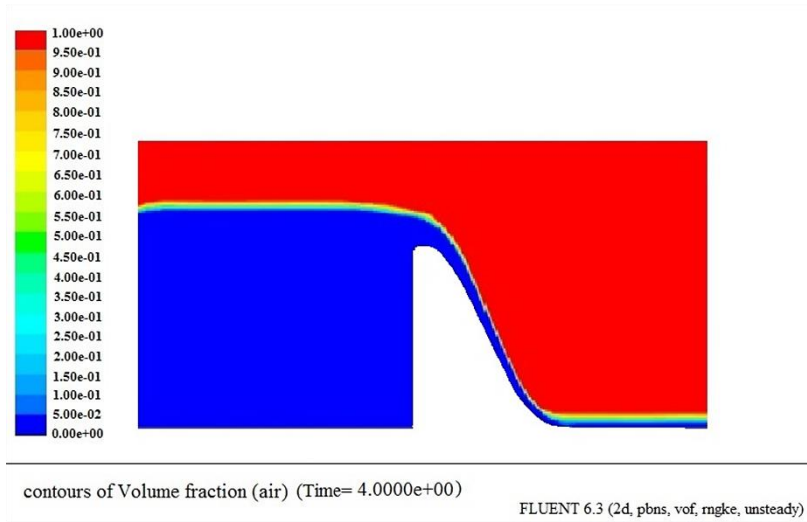


Figure 5. Ogee spillway water surface profile with a curvature radius of  $r/H_d = 2.5$  at 4s

### 3. Results

In Figures 6 to 8, the water surface profiles are given respectively for the  $Head/H_d$  ratios of 0.75, 1 and 1.5. In each of these Figures, analysis results are for different curvature radii. Specifications of the relevant inverse curves are given in the Figure guide. In this dimensionless ratio, parameter  $r$  represents the curvature radius of the inverse curve and  $H_d$  represents the water head of the spillway scheme.

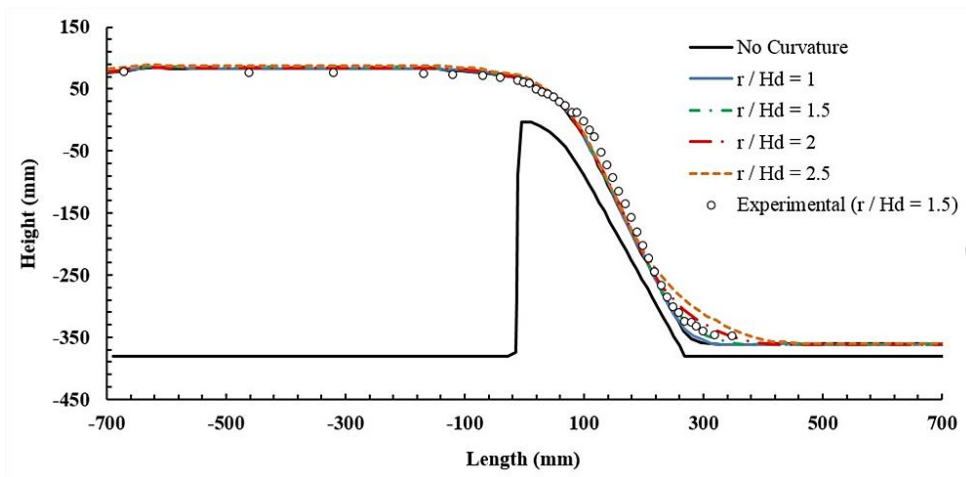


Figure 6. Comparison of the results of water surface profile for  $Head/H_d = 1.5$

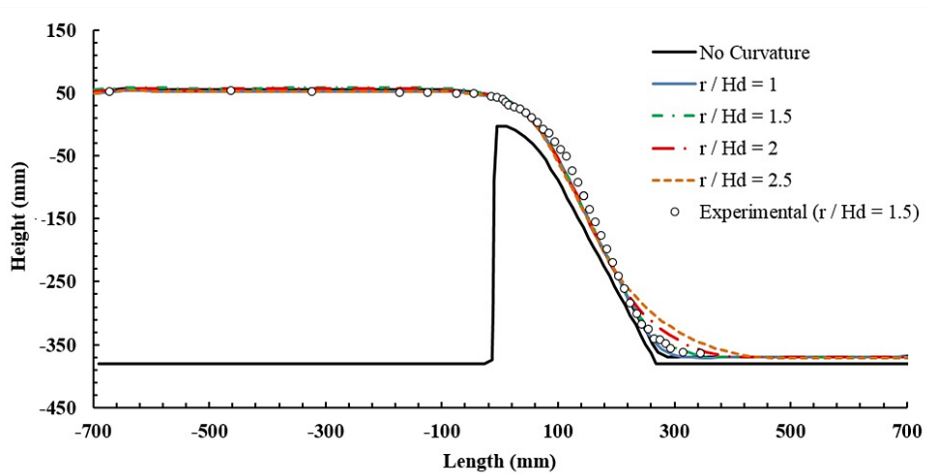


Figure 7. Comparison of the results of water surface profile for  $Head/H_d = 1$

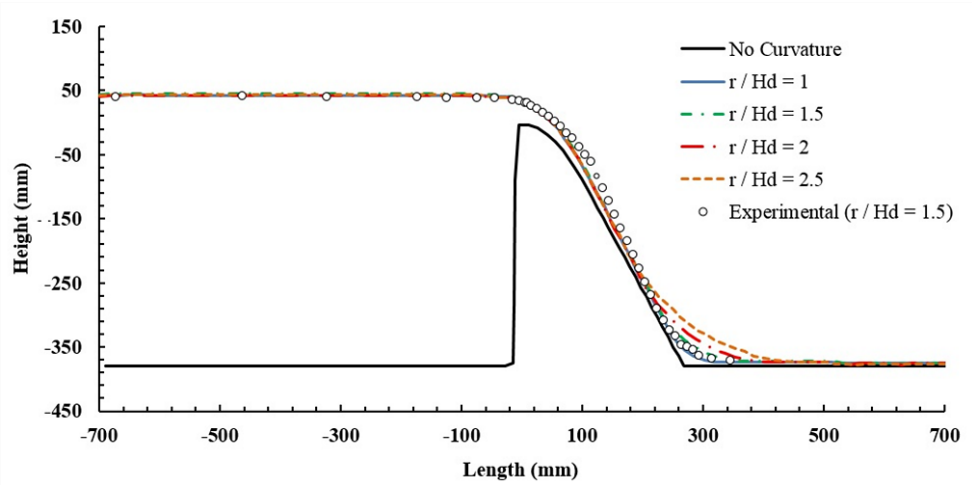


Figure 8. Comparison of the results of water surface profile for  $Head/H_d = 0.75$

According to the above figures, effect of changes in the radius of curvature can only be seen in the inverse curve area, and the other areas are unaffected. Experimental results of Chatila and Tabara (2004) are also provided in these Figures and a full compliance with the relevant numerical results is also evident. Radii of the inverse curves are shown with the dimensionless number of  $r/H_d$ . In Figure 9, absolute error values obtained from the numerical solution are provided with experimental results in three ratios of  $Head/H_d = 0.75, 1, 1.5$ . Absolute error values obtained with the negative sign mean lower value of the numerical solution compared with laboratory values. And error values with the positive sign indicate the higher amount of numerical solution compared with laboratory values.

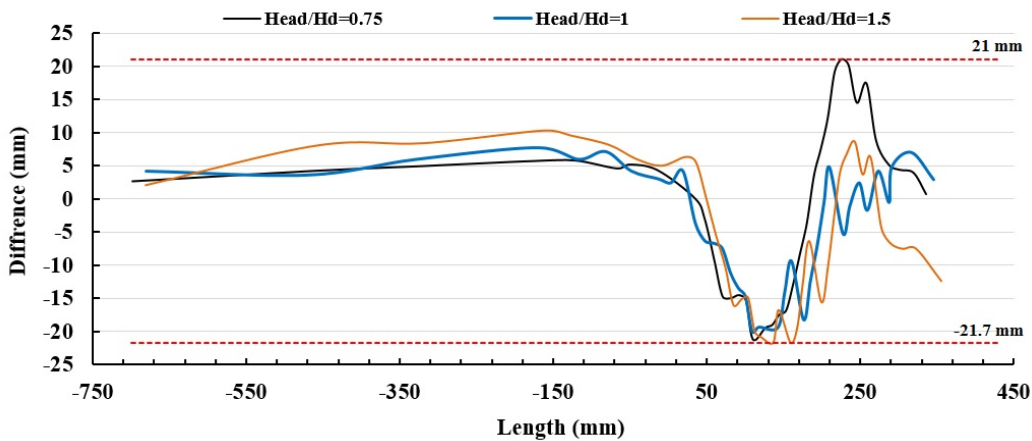


Figure 9. Differences between numerical and experimental  $Head/H_d$  ratios of 0.75, 1, 1.5.

It can be seen that the highest error of numerical results is for the  $Head/H_d$  ratio of 1.5 which is 21.7 mm less than the amount obtained in laboratory. Calculated difference indicates a good agreement between data and their proximity to one another. In Figures 10-12, results of the absolute pressure distribution versus the spillway height are presented. In Figures 10-12, both horizontal and vertical axes are dimensionless. The horizontal axis represents the absolute pressure ratio to the atmospheric pressure and the vertical axis indicates the spillway height which is normalized between 0 and 1. Zero represents the spillway crest height and the number (-1) indicates the toe height.

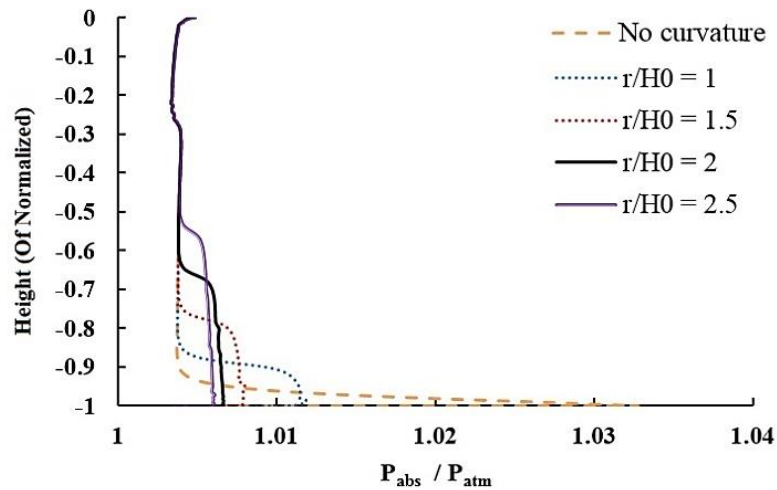


Figure 10. Comparison of the results of pressure distribution versus the spillway height for  $Head/H_d = 1.5$

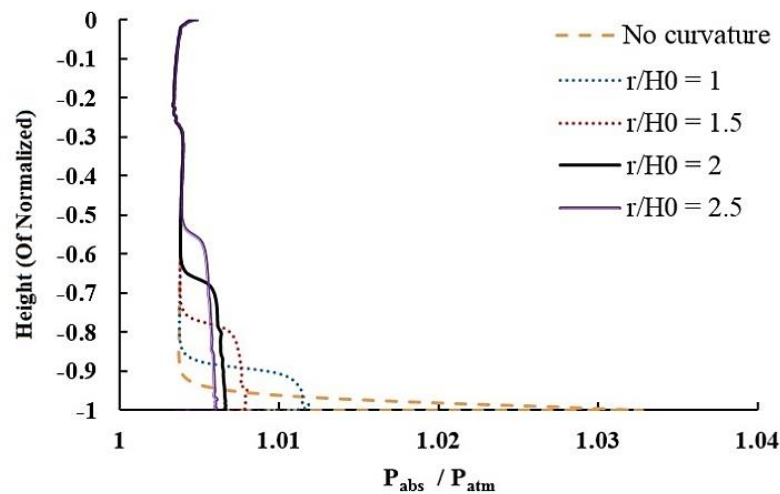


Figure 11. Comparison of the results of pressure distribution versus the spillway height for  $Head/H_d = 1$

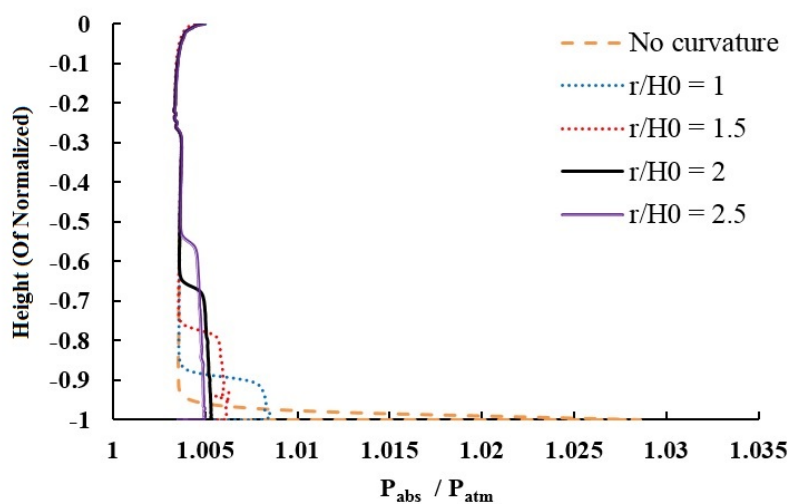


Figure 12. Comparison of the results of pressure distribution versus the spillway height for  $Head/H_d = 0.75$

According to Figures 10-12, need for inverse curve is always required because pressure dramatically increases in its absence, due to separation of flow lines from the curved surface and contact with air. By increasing the curvature radius of this curve, the pressure increase gradually decreases. For  $r/H_d$  of 2.5, the pressure is reduced 0.0246 atm. Increment in the value of  $Head/H_d$  compared to  $r/H_d$ , the pressure constant in the toe is increased and the effect of inverse

curvature on pressure reduction is decreased. In Figures 13 to 15, relationship between the maximum relative pressure and  $r/H_d$  are given. A quadratic polynomial equation were fitted to the relationships. Table 2 shows the details of the fitted equation and the corresponding regression coefficient

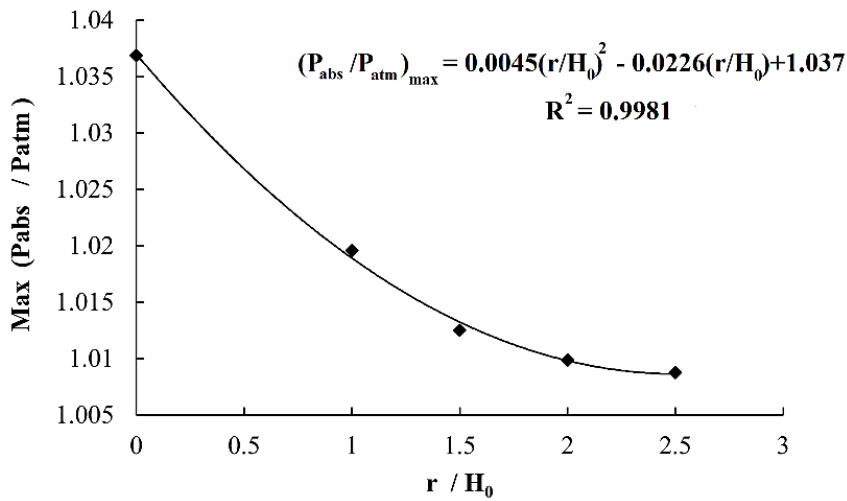


Figure 13. Changes in the maximum relative pressure versus the radius of curvature for  $Head/H_d = 1.5$

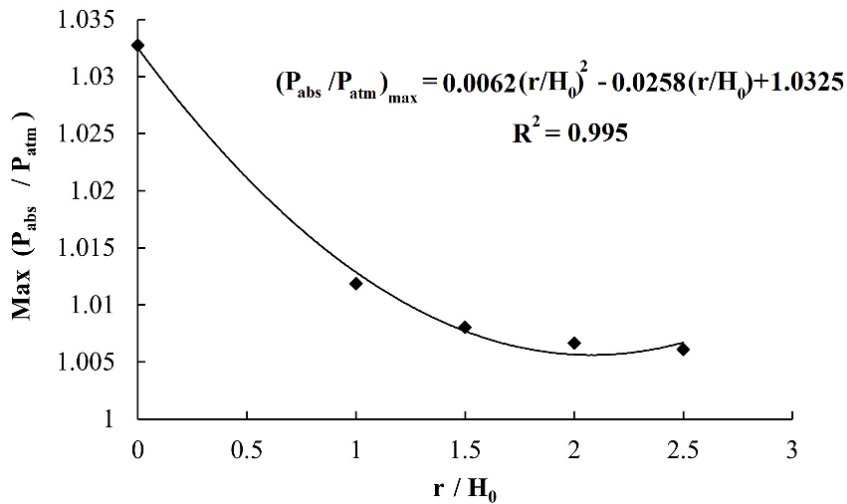


Figure 14. Changes in the maximum relative pressure versus the radius of curvature for  $Head/H_d = 1$

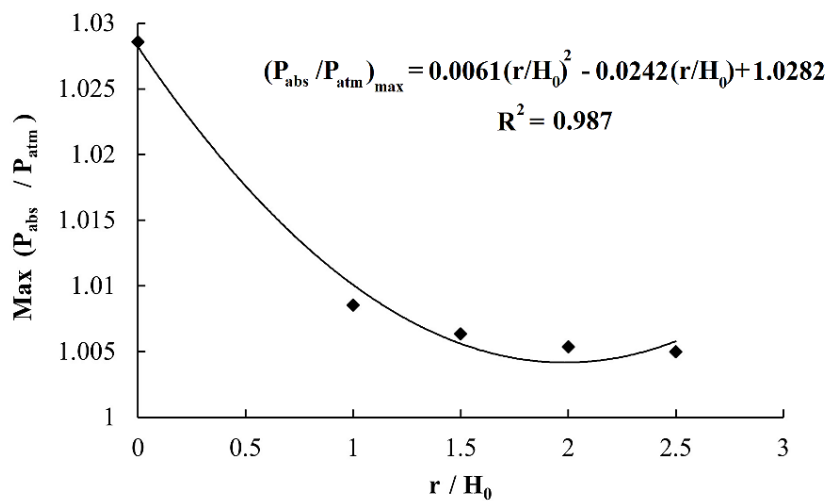


Figure 15. Changes in the maximum relative pressure versus the radius of curvature for  $Head/H_d = 0.75$

**Table 2. Specifications of the fitted equations and the corresponding correlation coefficient**

Head/ $H_d$	Equation	Correlation coefficient
1.5	$(P_{abs}/P_{atm})^2_{max} = 0.0045\left(\frac{r}{H_0}\right)^2 - 0.0226\left(\frac{r}{H_0}\right) + 1.037$	0.9981
1	$(P_{abs}/P_{atm})^2_{max} = 0.0045\left(\frac{r}{H_0}\right)^2 - 0.0258\left(\frac{r}{H_0}\right) + 1.0325$	0.9950
0.75	$(P_{abs}/P_{atm})^2_{max} = 0.0061\left(\frac{r}{H_0}\right)^2 - 0.0242\left(\frac{r}{H_0}\right) + 1.0285$	0.9874

Investigations on the Figures 13 to 15, show that:

- The maximum pressure on the inverse curve is reduced by increasing the radius of curvature.
- Pressure increment in zero curvature is caused by sudden collision of flow lines and turbulence caused by it. While by increase in inverse profile curvature, the turbulence is created in flow lines and therefore, the maximum pressure shows a lower value than before.

When  $Head/H_d$  ratio increases, the maximum pressure also increases which is reasonable.

#### 4. Conclusion

Here, the flow behavior on the ogee spillway is numerically simulated. 2 dimensional numerical simulation was performed by Fluent software, and turbulence model of RNGk- $\epsilon$  was used for modeling turbulences in the flow. The results of numerical solution were compared and validated by laboratory results obtained by Chatila and Tabara (2004). The highest error of numerical solution for the  $Head/H_d$  ratio of 1.5 was -21.7 mm demonstrating closeness of data and good agreement between the numerical and laboratory results. A dimensionless number was considered for introducing the inverse curvature of the arc which is the ratio of curvature radius to the spillway design ( $r/H_d$ ). In order to study the effect of inverse curvature on distribution of the spillway body pressure profile, four values were considered for the mentioned dimensionless number which are zero (without inverse curve), one (1), one and a half (1.5), two (2), and two and a half (2.5). Of course, it should be noted that each of these states were simulated for three different values of water head. Based on the surveys, an inverse curve is clearly essential because in its absence, the pressure on the spillway body increases at once in the toe area. By increasing the curvature radius of the inverse curve, this pressure increase is reduced; as in  $r/H_d = 2.5$ , the pressure is reduced by 2.46%. Some relationships are also provided to predict the pressure reduction relation. That's while the average pressure did not show significant changes at different values of curvature radius. It should be noted that the reduction of maximum pressure against increasing the curvature radius should be regarded with economic considerations. Because increasing the curvature radius of the inverse curve increases economic costs as well.

#### 5. References

- [1] Chanson, Hubert. "The Hydraulics of Open Channel Flow An Introduction". Elsevier Butterworth Heinemann, (2004): pp 496.
- [2] Bradley, Joseph N. "Studies of flow characteristics, discharge and pressures relative to submerged dams". Hydraulic Laboratory Rep. No. 182, (1945).
- [3] Cassidy, John J. "Irrotational flow over spillways of finite height". Journal of Hydraulic Engineering 91, no. 6 (1965): 155-173.
- [4] Maynard, Stephen T. "General spillway investigation". Tech. Rep. HL-85-1, U.S. Army Engineer Waterways Experiment Station, Vicksburg, Miss, (1985).
- [5] Savage, Bruce M., and Michael C. Johnson. "Flow over ogee spillway physical and numerical model case study". Journal of Hydraulic Engineering, ASCE 127, no. 8 (2001): 640-649. DOI: 10.1061/(ASCE)0733-9429(2001)127:8(640).
- [6] Chunrong, Liu, Huhe Aode, and Ma Wenju. "Numerical and experimental investigation of flow over a semicircular weir". Acta Mech Sinica 18, no.6 (2002): 594-602. DOI: 10.1007/BF02487961.
- [7] Chatila, Jean, and Mazen Tabbara. "Computational modeling of flow over an ogee spillway". Computers and Structures 82, no.22 (2004): 1805-1812. DOI: 10.1016/j.compstruc.2004.04.007.
- [8] Michael C. Johnson and Savage, Bruce M. "Physical and Numerical Comparison of Flow Over Ogee Spillway in the Presence of Tail water". Journal of Hydraulic Engineering 132, no. 12 (2006). DOI: 10.1061/(ASCE)0733-9429(2006)132:12(1353).
- [9] Tullis, Blake P. "Behavior of Submerged Ogee Crest Weir Discharge Coefficients". Journal of Irrigation and Drainage Engineering 137, no. 10 (2010): 677-681. DOI: 10.1061/(ASCE)IR.1943-4774.0000330.
- [10] Vosoughifar, Hamidreza, and Alireza Daneshkhah. "CFD and dimensionless parameter analysis of Froude number to determine

the flow regime over ogee spillways". *Journal of Water Sciences Research* 2, no. 1 (2010): 21-29.

- [11] Morales, Viviana, Talia E. Tokyay, and Marcelo Garcia. "Numerical Modeling of Ogee Crest Spillway and Tainter Gate Structure of a Diversion Dam on Canar River". Ecuador, XIX International Conference on Water Resources, (2012).
- [12] Alhashimi Drsam. "CFD Modeling of Flow over Ogee Spillway by Using Different Turbulence Models". *International Journal of Scientific Engineering and Technology Research* 2, no. 15 (2013): 1682-168.
- [13] Daneshfaraz Rasoul, Kaya Birol, Sadeghfam Sina and Sadeghi Hojat. "Simulation of Flow over Ogee and Stepped Spillways and Comparison of Finite Volume and Finite Element Methods". *Journal of Water Resource and Hydraulic Engineering* 3, no. 2 (2014): 37-47.
- [14] Herrera-Granados, Oscar, and Stanisław W. Kostecki. "Numerical and physical modeling of water flow over the ogee weir of the new Niedów barrage". *Journal of Hydraulic and Hydromechanic* 64, no. 1 (2016): 67–74. DOI: 10.1515/johh-2016-0013.
- [15] Daneshfaraz, Rasoul, Ali Rezazadeh Joudi, Ali Ghahramanzadeh, and Amir Ghaderi "Investigation of flow pressure distribution over a stepped spillway," *Advances and Applications in Fluid Mechanics* 19, no.4 (2016): pp.811–822. DOI: 10.17654/FM019040805.
- [16] Patankar, Suhas. "Numerical Heat Transfer and Fluid Flow". Hemisphere Publishing Corporation, Taylor & Francis Group, New York, (2012) pp. 11-23.
- [17] Dargahi, Bijan. "Experimental study and 3D numerical simulations for a free-overflow spillway." *Journal of Hydraulic Engineering* 132, no. 9 (2006): 899-907. DOI: 10.1061/(ASCE)0733-9429(2006)132:9(899).
- [18] Kim, Dae Geun, and Jae Hyun Park. "Analysis of flow structure over ogee-spillway in consideration of scale and roughness effects by using CFD model". *KSCE Journal of Civil Engineering* 9, no. 2 (2005): 161-169 .DOI: 10.1007/BF02829067.
- [19] Dehdar-Behbahani, Sadegh, and Abbas Parsaie. "Numerical modeling of flow pattern in dam spillway's guide wall. Case study: Balaroud dam, Iran." *Alexandria Engineering Journal* 55, no. 1 (2016): 467-473. DOI:10.1016/j.aej.2016.01.006.
- [20] Mansoori, Abbas, Shadi Erfanian, and Farhad Khamchin Moghadam. "A Study of the Conditions of Energy Dissipation in Stepped Spillways with  $\Lambda$ -shaped step Using FLOW-3D." *Civil Engineering Journal* 3, no. 10 (2017): 856-867. DOI: 10.28991/cej-030920.
- [21] Yakhot V, Orsarg SA, Thangam S, Gatski TB, Speziale CG. "Development of turbulence models for shear flows by a double expansion technique." *Physics of Fluids* 4, no. 7 (1992): 1510-1520. DOI: 10.1063/1.858424.